

# Post-Processing of Cerebrovascular Models after DTF-skeletonization

Tasnim Tabassum Nova<sup>1</sup>, Florian Thamm M.Sc.<sup>1</sup>, Leonhard Rist M.Sc.<sup>1</sup> and Prof. Dr.-Ing. habil. Andreas Maier<sup>1</sup>

<sup>1</sup> Friedrich-Alexander-University Pattern Recognition Lab,  
Erlangen, Germany.

Contributing authors: [tasnim.nova@fau.de](mailto:tasnim.nova@fau.de);  
[florian.thamm@fau.de](mailto:florian.thamm@fau.de); [leonhard.rist@fau.de](mailto:leonhard.rist@fau.de);  
[andreas.maier@fau.de](mailto:andreas.maier@fau.de);

## Abstract

Computed tomography angiography (CTA) is a popular modality of choice for detecting strokes. As it can generate highly resolved images with enhanced vessel visibility. But sometimes it is difficult to locate the exact location of a stroke because of the surrounding vessels and bones. A graph of the complete vessel tree can give the physicians an overview of the patient's vessel structure. With this motivation in mind, Thamm et al. [1] proposed a visualization pipeline that can produce a skeletonized image from a CTA image. However, the skeletonized images sometimes do not follow the actual anatomical structure of the vessels. In this report, we have analyzed the geometrical and structural shapes of skeletonized graph models of brain vessels and proposed solutions to reconstruct them according to the actual structure of the vessel tree.

**Keywords:** CTA, stroke, skeletonization

## 1 Introduction

A stroke is a life-threatening medical emergency that occurs when the blood supply to parts of the brain is interrupted or reduced, preventing brain tissue from getting oxygen and nutrients. This causes the brain cells to die in minutes [2]. A fast detection and treatment are essential in this scenario. Most of the

## 2 Post-Processing of Cerebrovascular Models after DTF-skeletonization

strokes occur in the middle cerebral artery that is connected to the Circle of Willis. In the Circle of Willis internal carotid arteries (form the anterior circulation) and the vertebral/basilar arteries (supply the posterior circulation) of the brain connect with each other. This place is surrounded by its peripheral vessels and other cerebral arteries [3][4].

To detect strokes, physicians need to visualize the actual vessel structure of the patients. Computed tomography angiography (CTA) is reported to be the most widely used modality for the detection of strokes because of its speed and ability to acquire the exact site of occlusion in the cerebral vessels [5]. However, for a better overview of the vascular system, it is needed to model it as a graph for 3D visualization. The graph and surface model is generated by applying the DTF-Skeletonization [6] to a segmentation of the vessel tree [1].

The main idea of skeletonization is to reduce the dimension of an object under consideration, so that this representation carries all information about the original shape of the object and, at the same time, facilitates an algorithmic geometrical and structural shape analysis [7][8][9][10]. Skeletonization has been widely used in different medical imaging applications. Because of the structure of the blood vessels, it has become a very useful tool to simplify the vessel tree.

Thamm et al. [1] applied skeletonization as a part of their proposed fully automated image processing and visualization pipeline, which provides a full segmentation and modeling of the cerebral arterial tree for CTA data. Their algorithm can automatically label the cerebral arteries (Middle Cerebral Artery left and right, Anterior Cerebral Artery short, Posterior Cerebral Artery left and right) and detect occlusions or interruptions in these vessels due to stroke. To detect the actual structure of vessel trees, it is important to compute a proper skeletonization. But in some regions, this computation may be difficult because a large number of neighboring vessels make loop structures in the skeletons. To avoid this, post-processing of the skeletonized images is needed.

In this report, we have discussed the loop structures in detail. We categorized the loops into two main groups: Type-01 and Type-02 and proposed a classifier to differentiate between them. We also discuss two methods to eliminate Type-01 loops.

## 2 Methodologies

### 2.1 Dataset

For this experiment, we used three datasets (001, 006 and 008). Each dataset consists of one CTA image of the cerebral arterial tree and one DTF-skeletonized image of that CTA image segmentation. We are mainly interested in the Sinus Sagittalis part. It is the largest blood vessel in the human brain and is located in the front to the middle area below the skullcap. Various veins flow into it and carry the blood to the upper layers of the brain tissue [11].

## 2.2 Types of Loop

The large vessels and surrounding small vessels of Sinus Sagittalis often make loop structures in the skeletonized CTA images. In Fig-1 and Fig-2, some examples of loops are shown.

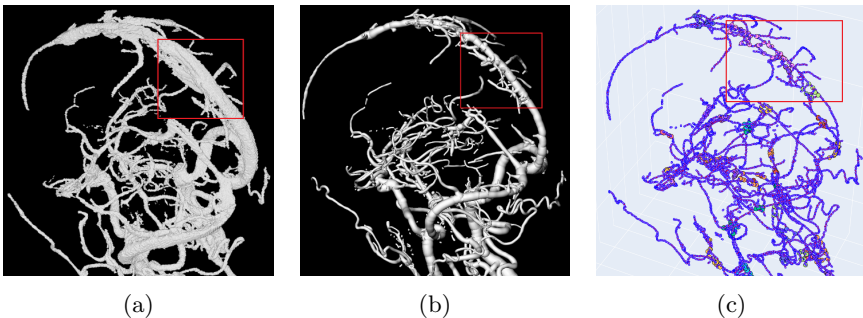


**Fig. 1:** Inside the red marked boxes, loops made from large vessels are shown; (a) Segmentation from CTA image, (b) Cerebrovascular model after DTF-skeletonized image, (c) Graph image

Fig-1 is taken from dataset 006. In the CTA image, a large vessel inside the red box can be seen. But in the skeletonized image, this large vessel breaks into some small loops. In the graph image, the node and edge structures of the loops can be visualized.

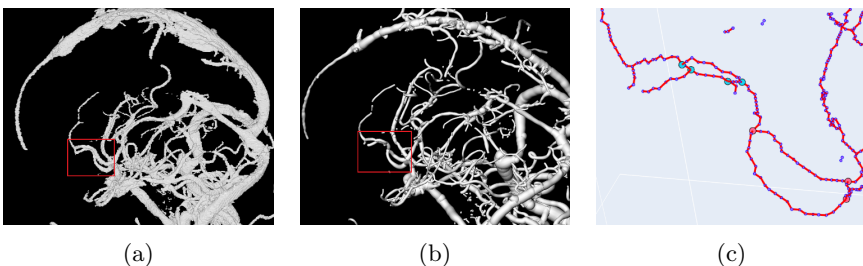


**Fig. 2:** Inside the red marked boxes, loops made by entanglement of two vessels are shown; (a) Segmentation from CTA image, (b) Cerebrovascular model after DTF-skeletonized image, (c) Graph image of the red marked boxes

Fig-2 is also taken from the same dataset 006. In the CTA image, we can see two vessels overlapping each other and making loops. Here loops are also visible in the CTA segmentation.

If we compare the two locations of the same graph (Fig-1c, Fig-2c), we notice that in Fig-1c nodes are densely located and the length of the edges is

small. Also, there are some noisy open edges. But in Fig-2c, nodes are sparsely located and edges are large compared to Fig-1c.

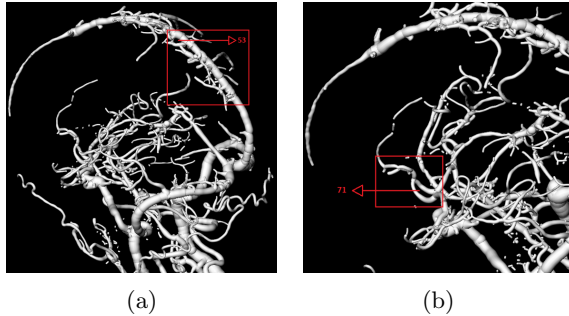


**Fig. 3:** Two loops (Loop number 53 and 71- marked with red arrow) are taken from dataset 006 for the comparison in Table-1

We calculated the average node density within one loop using the kernel density estimator and the total length of the edges of each loop. We took one loop from Fig-1b and another loop from Fig-2b (Marked with a red arrow in Fig-3) and compared their properties in Table-1.

**Table 1:** Loop Characteristic Comparison Table of Two Loops

Dataset	006	006
Loop no.	53	71
Average node density	$1.8 \times 10^{-6}$	$9.6 \times 10^{-7}$
Total loop length	3.3	9.3

Taking these two properties (Average node density and Total loop length) into account, we divide loops into two groups:

- **Type-01:** These loops have higher average node density and smaller total loop length.
- **Type-02:** These loops have lower average node density and larger total loop length

## 2.3 Loop Classifier

In order to eliminate these two types of loops, two different types of actions are needed to take. We designed a classifier to differentiate between these two groups. For this, we took two features:

1. **Average loop density:** Average density of the nodes within a loop by using kernel density estimator where kernel bandwidth = 10.

**2. Total loop length:** Total length of the edges within a loop.  
For classification, we used k-means clustering.

## 2.4 Elimination Procedure

### 2.4.1 Type-01 Loop elimination

As Type-01 loops are created from large vessels, here our main target was to merge all the loops and create edges that are aligned to the main direction of the vessel and have an enlarged radius. In the next two sections, we discuss two methods to eliminate Type-01 loops.

#### 2.4.1.1 Method-1

In order to describe the steps, one example cluster of Type-01 loop has been taken from dataset-006 (Fig-4).

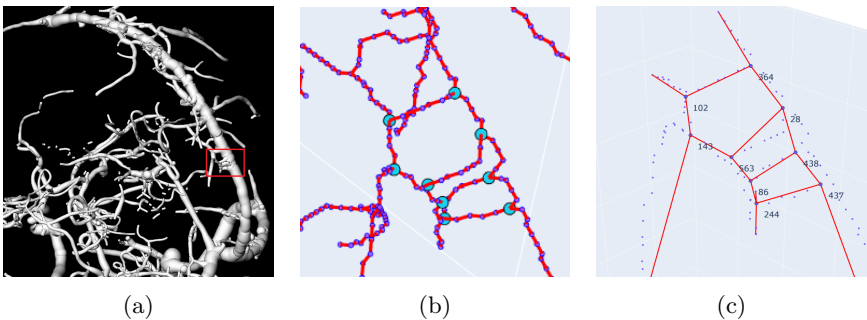


**Fig. 4:** One cluster from dataset 006 has been taken; (a) Cerebrovascular model after DTF-skeletonized image, (b) Graph image of the red marked box, (c) Graph image showing nodes (blue circles), edges (red lines) and skeletons (small blue circles)

This cluster has three loops, nine nodes (102, 364, 28, 438, 437, 244, 86, 563, 143), twelve internal edges ((102-364), (364-28), (28-438), (438-437), (437-244), (244-86), (86-563), (563-143), (143-102), (563-28), (86-438), (244-437)) and six external edges from (102, 364, 437, 244, 143) nodes. The elimination steps of the loops has been described in the following.

- **Step-1:** The edge which has the largest radius ( $r$ ) within this cluster is collected. This radius would be the final radius of the edges after modifications. In this example edge (28-438) has the largest radius.
- **Step-2:** Loop elimination starts from the loop which has the lowest number of nodes. In this example, loop [86, 244, 437, 438] has been selected.

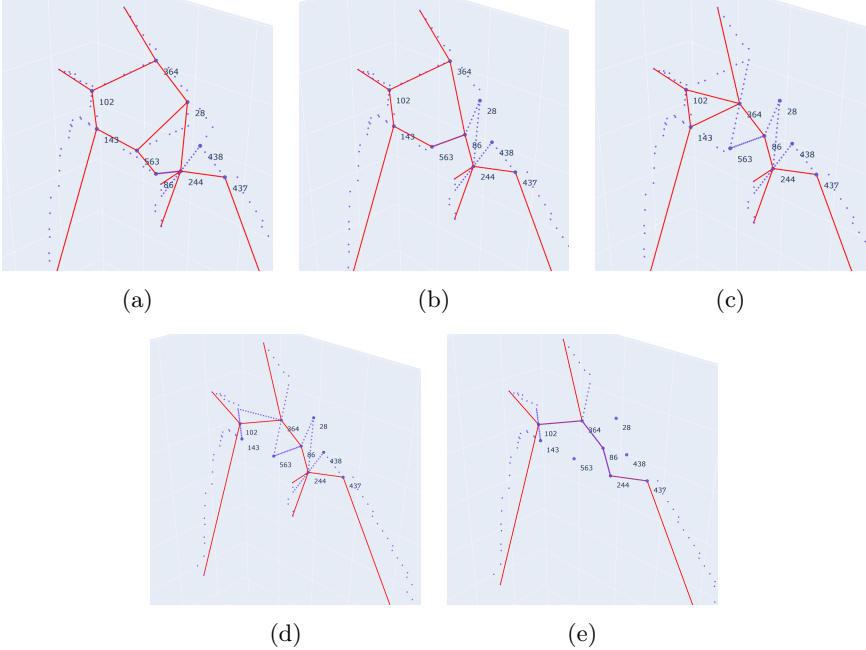


**Fig. 5:** Method-1: Type-01 Loop elimination process

- **Step-3:** From that loop, a corner is selected that has the smallest internal angle. In our case, it's with node 437 (Fig-5a). The edges ((437, 438), (437, 244)) that are connected to this node need to be modified.

The mid-distance between those two nodes (438, 244) is calculated. One node (node 244) is randomly selected from those two and the position of that node is modified to the calculated mid-distance. Here, the position of node 244 has been changed to the mid-distance of 244 and 438. All edges which are connected to the other node (438), would be connected to the selected node (244). The previous edges (438, 86), (438, 28), (438, 437) would be changed to (244, 86), (244, 28), (244, 437). As node 244 was previously connected to node 437, the new edges would create a two-node-loop. Node 438 should be deleted in the end.

The newly created two-node-loop needs to be eliminated. The elimination procedure of two-node-loops has been described in section 2.4.1.3. As node 244 is changing its position, we add some extra skeletons (blue dots in Fig-5a) to the edges which were connected to 244. Also, those edges which were connected to the deleted node would make some blank space. We fill those spaces with linearly connected skeletons.

The loop [86, 244, 437, 438] has been completely eliminated. Now the cluster has two more loops left (Fig-5a).

- **Step-4:** Step-2 and Step-3 are repeated until the loop cluster has any loop left (Fig-5b, 5c, 5d).
- **Step-5:** The remaining edges which were previously part of loops are selected. In this case, (437, 244), (244, 86), (86, 264), (264, 102). We fill the connecting lines of the predecessor and successor nodes with linearly connected skeletons (Fig-5e).
- **Step-6:** The radius of the remaining internal edges need to be modified with previously saved radius ( $r$ ).

We named this algorithm "Triangle Elimination Algorithm", as it always starts from one corner of the loop and eliminates the imaginary triangle. If two imaginary triangles can be fitted in a loop, then one step is needed to eliminate that loop.

#### 2.4.1.2 Method-2

The main idea of this method is taken from the path-finding robot algorithm. If we imagine that the loop cluster is the path for a robot and the robot starts moving from one node, then it will always move in the path which has a larger radius. To describe the steps, the same cluster has been used as an example like Method-1 (Fig-5).

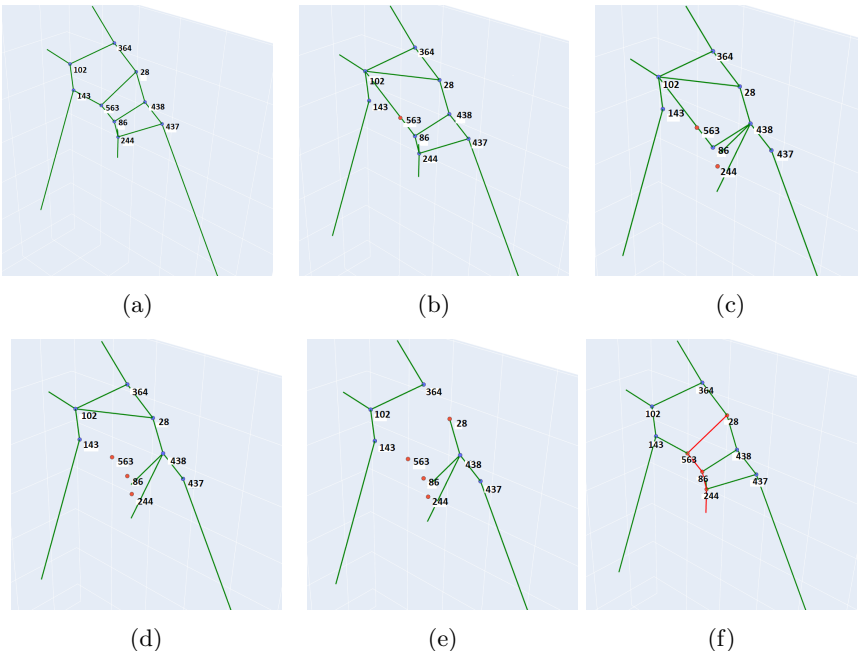


**Fig. 6:** Method-2: Type-01 Loop elimination process

- **Step-1:** This elimination procedure starts from the loop which has the highest number of nodes. In this example, loop [102, 364, 28, 563, 143] has been selected first.
- **Step-2:** A corner is selected from that loop that has the smallest angle. In this case, it's with node 143 (Fig-6a). Node 143 has two loop-making edges (143, 102) and (143, 563). Between these two edges, one edge is selected that has a larger radius than the other. In this case, it is the edge(143, 102). Edge (143, 563) and node 563 (Fig-6b, marked as red) need to be deleted. All the edges which are connected to 563 need to be connected to 102.
- **Step-3:** Step-01 and Step-02 need to be repeated until the loop cluster has any loop left.(Fig-6c, 6d, 6e). In (Fig-6e), all the loops are eliminated. The deleted nodes are marked as red in Fig-6e (node 563, 86, 244, 28).
- **Step-4:** All the edges (green edges) need to be retrieved that were connected to the remaining green nodes (143, 102, 364, 438, 437). Edges that were connected between two deleted nodes ((28, 563), (563, 86), (86, 244)) should be deleted in the end. Deleted edges are marked as red in Fig-6f.

#### 2.4.1.3 Two-node-loops

This type of loop has two nodes and two edges connected with each other. In other words, the loop-making edges have the same predecessor and successor nodes set (Fig-7a and 7b). A two-node-loop can be of Type-01 or Type-02 loop. In order to differentiate this, the same classifier (section 2.3 Loop Classifier) can be used. The elimination steps of Type-01 two-node-loops are described in the following.

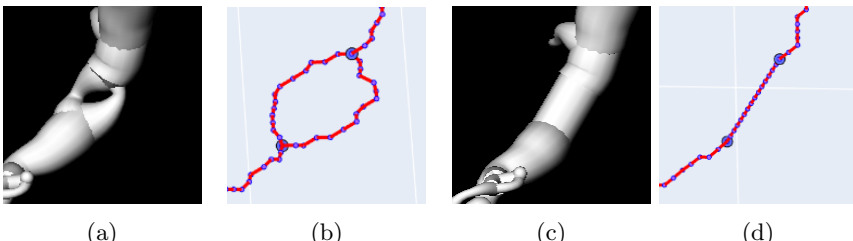


**Fig. 7:** Two-node-loops: example and elimination (a) DTF-skeletonized image before loop elimination, (b) Graph image before loop elimination, (c) DTF-skeletonized image after loop elimination, (d) Graph image after loop elimination

- **Step-1:** The number of skeletons of two edges are collected. The skeletons positions and the radius of that edge that has a higher number of skeletons (N-skeletons) need to be modified. And the other edge needs to be deleted.

- **Step-2:** Linear interpolation is performed between the predecessor and successor nodes. The number of interpolated points should be equal to N-skeletons.
- **Step-3:** The external edges that are connected to the predecessor and successor nodes are collected. One edge for each node is selected that has the highest radius. An average of them is taken and the radius of the previously modified edge is changed.

In Fig-7c and 7d, the result after the elimination procedure has been shown.

## 2.4.2 Type-02 Loop Elimination

### 2.4.2.1 Type-02 Loop Structure Analysis

Type-02 loops usually have three main node-sets (Fig-8). One set of nodes is at the starting point of the vessels which are always connected and should be connected after loop elimination.

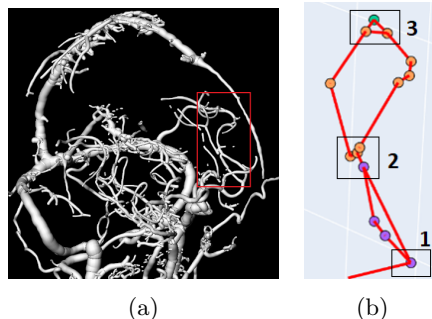


**Fig. 8:** Typical structure of Type-02 loops; (a) Cerebrovascular model after DTF-skeletonized image, (b) Graph image of the red marked box showing nodes and edges

Some nodes are responsible for connecting the middle portion of the crossing area of the vessels. These nodes are also always connected to create Type-02 loops but this connection should be removed after loop elimination.

Another set of nodes could be present at the ending point of those two vessels. These nodes are connected to create another Type-02 loop. This connection should also be removed during loop modification.

But all Type-02 loops do not follow this structure. Sometimes, vessels are so entangled that not possible to decide which nodes should be deleted and which one should be kept. An example is shown in Fig-9.

As Type-02 loops are made of two overlapping vessels, after eliminating the loops, we would get two separate vessels.

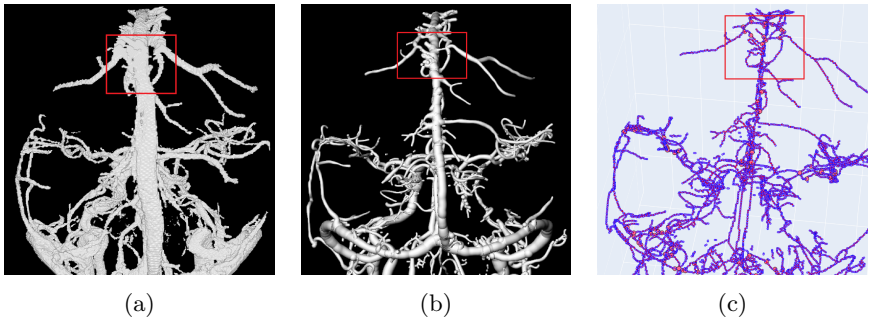


**Fig. 9:** Example of Type-02 loop which does not follow the typical structure

## 3 Results

### 3.1 Loop Classifier

In Fig. 10 a scatter plot of two loop feature: Total Loop Length and Average Loop Density of dataset 006 is shown. After applying the classifier, we got two clusters - blue cluster is for Type-01 loops and red one is for Type-02 loops.

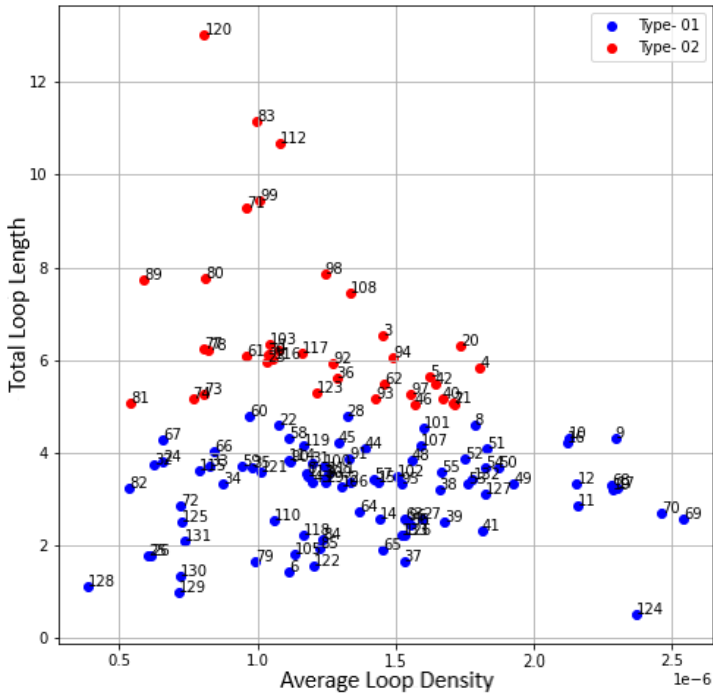


**Fig. 10:** Scatter plot of two loop features: Total Loop Length and Average Loop Density of dataset 006

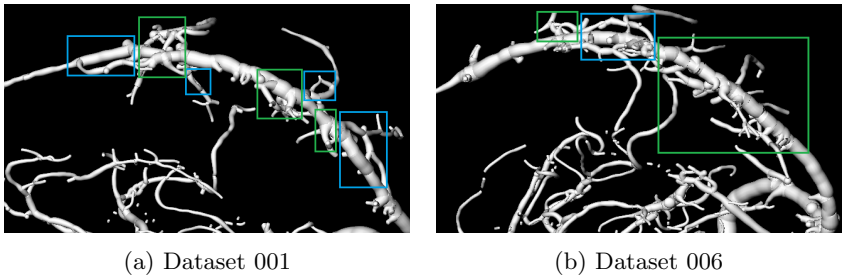


**Fig. 11:** DTF-skeletonized image of Sinus Sagittalis- Loops within the green boxes are correctly classified as Type-01 loops and loops within the blue boxes are correctly classified as Type-02 loop

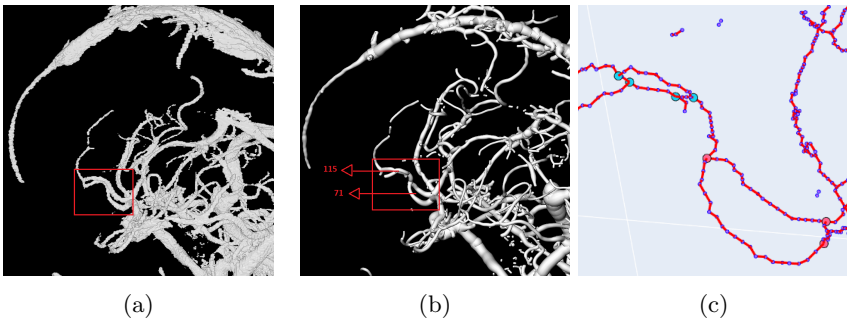


**Fig. 12:** Example of misclassification by the proposed classifier; Here Type-02 loop 115 has been detected as Type-01 loop

The classifier can successfully detect most of the loops in Sinus Sagittalis. In Fig-11 the Sinus Sagittalis of two datasets (001 and 006) are shown. Loops within the blue and green boxes are correctly classified.

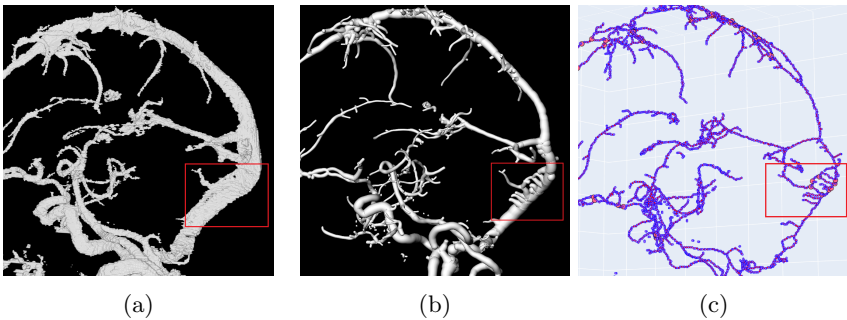
The loop classifier sometimes misclassifies loops. In Fig-12 and Fig-13, two examples are shown. Fig-12 is taken from dataset 006. Here, both 71 and 115 loops are Type-02 loops. The classifier successfully classifies 71 as Type-02 but it classifies 115 as Type-01 loop.

Fig-13 is taken from dataset 001. Loops within the red marked boxes are Type-01 loops but the classifier detects them as Type-02 loops.

### 3.2 Type-01 loop Elimination methods

Method-1 and Method-2 loop elimination processes have been applied to all the Type-01 loops in Sinus Sagittalis of dataset 006. Results are shown in Fig-14.

Method-1 is designed to eliminate all the loops of the selected region. But with this method, it is difficult to retrieve the original structure of the skeleton. Also, there might be some disjointed or twisty edges (Fig-14b).



**Fig. 13:** Example of misclassification by the proposed classifier; Loops inside the red box are Type-01 loops but they are detected as Type-02 loops by the classifier

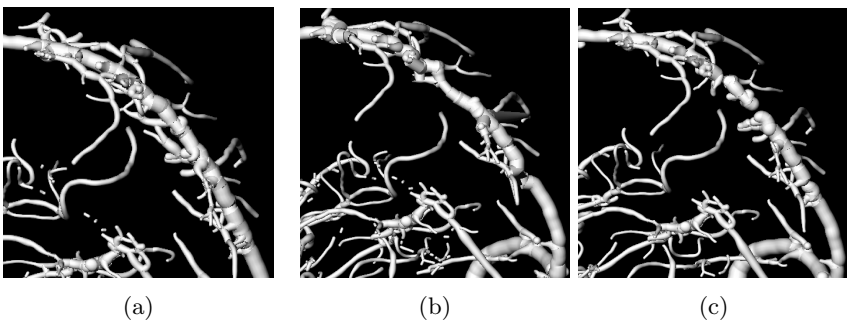


**Fig. 14:** Results after applying Type-01 loop elimination methods; (a) Original DTF-skeletonized image, (b) After applying Method-1 elimination method on Sinus Sagittalis region, (c) After applying Method-2 elimination method on Sinus Sagittalis region

Method-2 stores the original structure of the skeleton graph. But there might be some disconnected edges and also some small loops might remain in the end (Fig-14c).

## 4 Discussion

In this report, we have analyzed the loop-like structures in the DTF-skeletonized CTA brain vessel images. We divided these loops into two groups - Type-01 and Type-02 and proposed a classifier to categorize these two types of loops. The classifier takes “Average loop density” and “Total loop length” as features. The performance of the classifier is satisfactory. It can successfully classify most of the loops in the Sinus Sagittalis region. But it sometimes misclassifies loops that don’t follow the assumed characteristics (Section 2.2) of Type-01 and Type-02 loops. For better performance, one more feature like

surface areas of the loops or distance between two unconnected nodes in a loop could be added to the classifier.

We have also discussed the elimination process of Type-01 loops in this report. We have proposed two methods for the elimination. But none of these methods are working perfectly. Both of them have their advantages and disadvantages. Method-1 keeps the continuity of the connected edges. But it changes the actual structure of the vessels. On the other hand, Method-2 retains the original structures of the vessels but it might remove some important vessels.

In this report, we have not proposed any elimination process for Type-02 loops. This would be in our future work.

## 5 Conclusion

In this work, we have presented a detailed analysis of artificial loop-like structures in the skeletonized graph models of brain vessels. We observed that these loops can be distinguished into two main groups- Type-01 and Type-02. We proposed a classifier to differentiate between these two. We also proposed two methods to eliminate Type-01 loops. However, more work needs to be done to make these elimination processes robust.

## References

- [1] Thamm, F., Jürgens, M., Ditt, H., Maier, A.: Virtualdsa++: Automated segmentation, vessel labeling, occlusion detection and graph search on ct-angiography data. Eurographics Workshop on Visual Computing for Biology and Medicine (2020)
- [2] Wittenauer R., S.L.: Background paper 6.6 ischaemic and haemorrhagic stroke. priority medicines for europe and the world. a public health approach to innovation (2012)
- [3] Tissue plasminogen activator for acute ischemic stroke. The New England Journal of Medicine **333**, 1581–7 (1995)
- [4] Early stroke treatment associated with better outcome. the NINDS rt-PA stroke study. Neurology **55**, 1649–55 (2000)
- [5] Aviv RI, M.S.C.S.S.D.T.G.S.S.F.A. Shelef I: Early stroke detection and extent: impact of experience and the role of computed tomography angiography source images. Clin Radiol **62**, 447–52 (2007)
- [6] Selle, D.: Analyse von gefäßstrukturen in medizinischen schichtdatensätzen für die comutergestützte operationsplanung. PhD thesis (2000)
- [7] D.Ballard, C.Brown: Computer vision. Prentice-Hall **Chap. 8** (1982)

- [8] Davies, E.: Machine vision: Theory, algorithms and practicalities. Academic Press, 149–161 (1990)
- [9] Haralick, R., Shapiro, L.: Computer and robot vision. Addison-Wesley Publishing Company **Vol-1** (1992). Chap. 5
- [10] Jain, A.: Fundamentals of digital image processing. Prentice-Hall **Chap. 9** (1989)
- [11] Letchuman, V., Donohoe, C.: Neuroanatomy, superior sagittal sinus (2022)